Analysis on the shielding effect of elastic waves with infilled cavity rows by multiple scattering method

Chengwu Jiang[1], M. Sun[1*], X. Wei[1], Y. Dong[1], X. Wang[1], L. Zhou[1]

[1] Department of Civil Engineering, Zhejiang University City College, Hangzhou, 310015, China

ABSTRACT

Based on Biot's poroelastic theory and the multiple scattering method, it is obtained the theoretical solutions of plain P waves multiple scattered by arbitrarily arranged infilled cavity rows as barrier in saturated soil. Undetermined complex coefficients are achieved by expanding wave functions with the cavities-soil stress and displacement boundary conditions. Therefore, the solution of total wave field is confirmed before and after the barrier. The numerical examples have been manipulated to investigate the variation isolation effect trend of the cavity rows with the parameters such as scattering orders, intervals between infilled cavities and row spacing of barriers etc. Thus the optimum design proposals with rows of infilled cavities are acquired.

Keywords: multiple scattering; elastic wave; infilled cavity rows; discontinuous barriers

1 INTRODUCTION

With the development of urban area, the vibration induced by construction, vehicles and metro has become a serious problem to the residents. It not only damages the adjacent buildings, underground pipeline and precise equipment, but also influences citizens' daily life indirectly. Thus, studying how to reduce the influence of artificial vibration to urban environment has already become a major issue in soil dynamics for engineers and researchers.

For isolating artificial vibration, the continuous barriers and discontinuous barriers have been used worldwide. The infilled cavity rows, which are necessity of excavating open trenches or continuous walls, bringing a lot convenience to construction and support, meanwhile, saving more materials and costing less than continuous piles, are the most representative methods in discontinuous barriers. As the research foundation, elastic waves' refraction and reflection on the cylindrical interface have been studied for decades [1-4]. Cai et al. [5-6] solved the refraction of elastic waves by one row of piles in poroelastic soil theoretically. Xu et al. [7-8] adopted the conformal mapping method of complex functions to study the isolation effect to plane waves by pile rows and honeycomb cavities. Xia et al. [9-10] employed a more integrated Fourier-Bessel series function expansion to study the elastic wave scattering in vibration isolation barrier. Lu et al. [11-12] proposed linked periodic pile rows and developed a numerical model for simulating dynamic response. Sun et al. [13-14] using wave function expansion method to obtain the theoretical solutions of plain waves multiple scattering by rows of empty cavities with arbitrarily arranged based on Biot's saturated soil wave theory.

However, most of the above-mentioned researches are just focused on the single-phase medium, which is not conforming to the existing physical process of solid-liquid coupled scattering between soil skeleton and fluid in saturated soil. It is rarely analyzed elastic waves' coherence scattering in saturated media after meeting several infilled cavities with disordered orientation. Thus, this paper mainly concentrates on the shielding effect of elastic waves by infilled cavity rows, with the purpose of providing references for practical engineering application.

2 METHODOLOGY

2.1 Theoretical Model

The theoretical model used to calculate plane waves' multiple scattering by several diverse radius and random array of heterogeneity is shown in Ref. [10]. By replacing heterogeneity with infilled cavity rows, and assuming surrounding medium is saturated soil, a model diagram is displayed in Fig. 1.

While P-waves entering through the saturated medium, the coupling scattering phenomenon will take place so that it produces three kinds of scattering waves including compressional fast P-wave P_1, compressional slow P-wave P_2 and shear wave S. Considering the P_2 waves attenuating rapidly in saturated soil so that they are ignored and only the effect of P_1 waves are considered. Expanding the wave potential function of incident wave P into Fourier-Bessel series as cylindrical coordinate system:

$$ {}_{\mathrm{s}}^{o}\phi^{\mathrm{inc}} = \mathrm{e}^{\mathrm{i}\alpha_{1\mathrm{s}} r_{12}(\theta_1+\theta_{12})} \sum_{n=-\infty}^{+\infty} \mathrm{J}_n(\alpha_{1\mathrm{s}} r_o)\mathrm{e}^{\mathrm{i}n\varphi_o}\mathrm{e}^{-\mathrm{i}\omega t} \tag{1} $$

Where the right superscript inc of ϕ expresses incident wave, the left subscript s means soil skeleton, the left superscript o

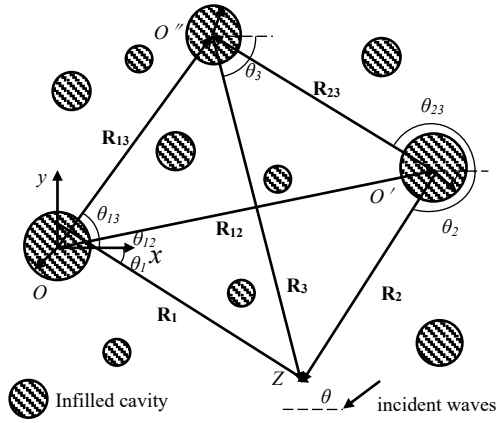

Fig. 1. 2-D model of plain P waves' multiple scattering by arbitrarily arranged infilled cavities barrier in saturated soil

represents the oth infilled cavity. $J_n(\cdot)$ is an nth-order Bessel function, α_{1s} shows the wavenumbers of incident P-waves, where subscript 1 means P_1 waves and subscript s expresses soil, $\varphi_o=\theta_o+\theta+\pi/2$.

As for cylindrical heterogeneities, the displacement potential function of scattering waves can be expressed as the series forms:

$$ {}_{\mathrm{s}}^{o}\phi_m^{\mathrm{sc}} = \sum_{n=-\infty}^{+\infty} {}^{o}A_m \mathrm{H}_n(\alpha_{1\mathrm{s}} r_o)\mathrm{e}^{\mathrm{i}n\theta_o} \tag{2a} $$

$$ {}_{\mathrm{f}}^{o}\phi_m^{\mathrm{sc}} = \sum_{n=-\infty}^{+\infty} {}^{o}B_m \mathrm{H}_n(\alpha_{2\mathrm{s}} r_o)\mathrm{e}^{\mathrm{i}n\theta_o} \tag{2b} $$

$$ {}^{o}\psi_m^{\mathrm{sc}} = \sum_{n=-\infty}^{+\infty} \mathrm{i}\,{}^{o}C_m \mathrm{H}_n(\beta_{\mathrm{s}} r_o)\mathrm{e}^{\mathrm{i}n\theta_o} \tag{2c} $$

$$ {}^{o}\chi_m^{\mathrm{sc}} = \xi_{11}\,{}_{\mathrm{s}}^{o}\phi_m^{\mathrm{sc}} + \xi_{12}\,{}_{\mathrm{f}}^{o}\phi_m^{\mathrm{sc}} \tag{2d} $$

$$ {}^{o}\Theta_m^{\mathrm{sc}} = \xi_{13}\,{}^{o}\psi_m^{\mathrm{sc}} \tag{2e} $$

Where ψ represents scattering S-waves potential function, the right superscript sc expresses scattering P-waves. The left subscript s and f means soil skeleton and fluid in the soil medium respectively. The subscript 2 in α_{2s} means P_2 wavenumbers in fluid. β_s expresses scattering SV wavenumbers. A, B and C represents undetermined complex coefficients. The subscript m means the mth scattering. $H_n(\cdot)$ is an nth-order Hankel function of the first kind. ${}^{o}\chi_m^{\mathrm{sc}}$ and ${}^{o}\Theta_m^{\mathrm{sc}}$ are composed by scattering wave potential of ${}_{\mathrm{s}}^{o}\phi_m^{\mathrm{sc}}$, ${}_{\mathrm{f}}^{o}\phi_m^{\mathrm{sc}}$ and ${}^{o}\psi_m^{\mathrm{sc}}$, ξ_{11}, ξ_{12} and ξ_{13} indicates the coupling coefficients.

As for infilled cavity, the incidence of P-waves will also produce coupling transmitted waves, which composed with P_1, P_2 and SV waves. Thus the displacement potential function of transmitted waves can be shown as the series forms:

$$ {}_{\mathrm{s}}^{o}\phi_m^{\mathrm{t}} = \sum_{n=-\infty}^{+\infty} {}^{o}D_m \mathrm{H}_n(\alpha_{1\mathrm{p}} r_o)\mathrm{e}^{\mathrm{i}n\theta_o} \tag{3a} $$

$$ {}_{\mathrm{f}}^{o}\phi_m^{\mathrm{t}} = \sum_{n=-\infty}^{+\infty} {}^{o}E_m \mathrm{H}_n(\alpha_{2\mathrm{p}} r_o)\mathrm{e}^{\mathrm{i}n\theta_o} \tag{3b} $$

$$ {}^{o}\psi_m^{\mathrm{t}} = \sum_{n=-\infty}^{+\infty} \mathrm{i}\,{}^{o}F_m \mathrm{H}_n(\beta_{\mathrm{p}} r_o)\mathrm{e}^{\mathrm{i}n\theta_o} \tag{3c} $$

$$ {}^{o}\chi_m^{\mathrm{t}} = \xi_{21}\,{}_{\mathrm{s}}^{o}\phi_m^{\mathrm{t}} + \xi_{22}\,{}_{\mathrm{f}}^{o}\phi_m^{\mathrm{t}} \tag{3d} $$

$$ {}^{o}\Theta_m^{\mathrm{t}} = \xi_{23}\,{}^{o}\psi_m^{\mathrm{t}} \tag{3e} $$

Where the right superscript t indicates transmitted waves, D, E, F represent transmitted coefficients of the oth-cavity respectively, ξ_{21}, ξ_{22} and ξ_{23} indicates the wave coupling coefficients. The rest of the symbols have the same significance as before.

2.2 Model Solution

The stress boundary condition of the first order scattering is continuous:

$$ \left[u_{r_o}^{\mathrm{inc}}(r_o,\theta_o) + {}^{o}u_{1r_o}^{\mathrm{sc}}(r_o,\theta_o)\right]\Big|_{r_o=a_o} = {}^{o}u_{1r_o}^{\mathrm{t}}(r_o,\theta_o)\Big|_{r_o=a_o} \tag{4a} $$

$$ \left[u_{\theta_o}^{\mathrm{inc}}(r_o,\theta_o) + {}^{o}u_{1\theta_o}^{\mathrm{sc}}(r_o,\theta_o)\right]\Big|_{r_o=a_o} = {}^{o}u_{1\theta_o}^{\mathrm{t}}(r_o,\theta_o)\Big|_{r_o=a_o} \tag{4b} $$

$$ \left[{}_{\mathrm{f}}w^{\mathrm{inc}}(r_o,\theta_o) + {}_{\mathrm{f}}^{o}w_1^{\mathrm{sc}}(r_o,\theta_o)\right]\Big|_{r_o=a_o} = {}_{\mathrm{f}}^{o}w_1^{\mathrm{t}}(r_o,\theta_o)\Big|_{r_o=a_o} \tag{4c} $$

The boundary stress at the interface of soil and fluid is also continuous:

$$ \left[\sigma_{r_o r_o}^{\mathrm{inc}}(r_o,\theta_o) + {}^{o}\sigma_{1r_o r_o}^{\mathrm{sc}}(r_o,\theta_o)\right]\Big|_{r_o=a_o} = {}^{o}\sigma_{1r_o r_o}^{\mathrm{t}}(r_o,\theta_o)\Big|_{r_o=a_o} \tag{5a} $$

$$ \left[\sigma_{r_o\theta_o}^{\mathrm{inc}}(r_o,\theta_o) + {}^{o}\sigma_{1r_o\theta_o}^{\mathrm{sc}}(r_o,\theta_o)\right]\Big|_{r_o=a_o} = {}^{o}\sigma_{1r_o\theta_o}^{\mathrm{t}}(r_o,\theta_o)\Big|_{r_o=a_o} \tag{5b} $$

$$ \left[{}_{\mathrm{f}}p^{\mathrm{inc}}(r_o,\theta_o) + {}_{\mathrm{f}}^{o}p^{1}(r_o,\theta_o)\right]\Big|_{r_o=a_o} = 0 \tag{5c} $$

o=0, 1, 2,…N, $0\le\theta_o\le 2\pi$

In the cylindrical-coordinate system, the potential equation of soil skeleton and fluid stress can be acquired by substituting the equilibrium equation of Biot's poroelastic theory [15]. Accordingly, it expresses the first order of scattering as a matrix **QX**=**R**, in which **Q** is the scattering and transmitted matrix, **X** is the first order of undetermined scattering and transmitted coefficient matrix, **R** is a vector of the incident waves.

$$ \sum_{n=-\infty}^{+\infty} \begin{bmatrix} q_{11} & q_{12} & \mathrm{L} & q_{1j} \\ q_{21} & q_{22} & \mathrm{K} & q_{2j} \\ \mathrm{M} & \mathrm{M} & \mathrm{O} & \mathrm{M} \\ q_{i1} & q_{i2} & \mathrm{L} & q_{ij} \end{bmatrix} \mathbf{X} = -\,{}^{o}\theta_{\alpha} \sum_{n=-\infty}^{+\infty} \begin{bmatrix} r_1 \\ r_2 \\ \mathrm{M} \\ r_i \end{bmatrix} \tag{6} $$

Setting up the subscripts i and j of the elements q, r for i=1, 2, … , 6; j=1, 2, … , 6; the first order of scattering and transmitted coefficients are $\mathbf{X}=|\mathbf{Q}_i/\mathbf{Q}|$.

Secondly, the m-th ($m\ge 2$) scattering satisfied the elastic boundary conditions similarly as the first scattering, and the iteration relationship between mth and (m-1) th order of scattering can be obtained as **QX=SY**.

$$ \sum_{n=-\infty}^{+\infty} \begin{bmatrix} q_{11} & q_{12} & \mathrm{L} & q_{1j} \\ q_{21} & q_{22} & \mathrm{L} & q_{2j} \\ \mathrm{M} & \mathrm{M} & \mathrm{O} & \mathrm{M} \\ q_{i1} & q_{i2} & \mathrm{L} & q_{ij} \end{bmatrix} \mathbf{X} = -\sum_{o'=0,o'\neq o}^{N'} \sum_{n'=-\infty}^{+\infty} \sum_{n=-\infty}^{+\infty} \begin{bmatrix} s_{11} & s_{12} & \mathrm{L} & s_{1j} \\ s_{21} & s_{22} & \mathrm{L} & s_{2j} \\ \mathrm{M} & \mathrm{M} & \mathrm{O} & \mathrm{M} \\ s_{i1} & s_{i2} & \mathrm{L} & s_{ij} \end{bmatrix} \mathbf{Y} \tag{7} $$

In which **X** is the m-th order of undetermined scattering and transmitted complex coefficient matrix, **Y** is the (m-1) th order of scattering and transmitted coefficients matrix, **Q** has the same meaning as the above mentioned and **S** is a vector. Accordingly, the solution of total wave field can be obtained by generalized Graf's addition theory [10].

3 NUMERICAL MODELS

Adopted the same numerical model of Avilés [2], the

eight infilled cavities can be arranged into two kinds of form: the linear and the hexagon type as shown in Fig. 2.

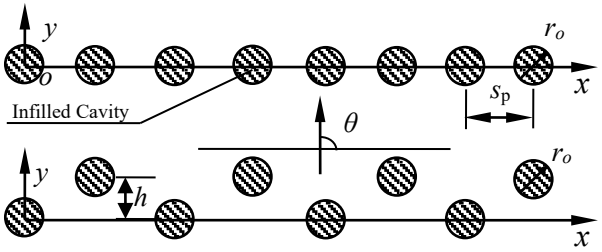

Fig 2. Linear single-row arrangement and hexagon double-row arrangement of infilled cavity barrier

$$\zeta_{ps} = 2a_s / \Lambda_{ps} = \alpha_{1s} a_o / \pi \quad (8a)$$

$$\zeta_{pf} = 2a_s / \Lambda_{pf} = \alpha_{2s} a_o / \pi \quad (8b)$$

$$\zeta_{ss} = 2a_s / \Lambda_{ss} = \beta_s a_o / \pi \quad (8c)$$

The definition of parameter ζ and Λ refer to [14], and the dimensionless displacement amplitude $|u/u_0|$ represents the total displacement amplitude of scattered waves over incident waves. The physical mechanical parameters are shown in Table 1, where the infilled fluid is pure water [3].

Table 1. Biot parameters in saturated soil

parameter	value
λ / GPa	7.556
G / 10^{-2}Pa	2.61
ρ_f (kg/m^3)	1000
η	0.94
M_1 (GPa)	7.407
ρ_1 (kg/m^3)	2204.5
ζ_{ps}	0.45
ζ_{pf}	0.8
ζ_{ss}	0.6

4 RESULTS AND DISCUSSIONS

4.1 The effect of scattering orders

It can be observed from Fig. 3 that the total variation trend of dimensionless displacement amplitude maintains consistent with the total variation trend behind the emptied cavities rows in reference [14]. With the addition of scattering order m, $|u/u_0|$ enlarges gradually and the amplification also decreases gradually which is convergent. It comes in small increment when the m values is 4, which means that adopting multiple scattering hypothesis is convincible and it can use m=4 to design barriers in practice. Secondly, it can be observed that the displacement amplitude reaches at a distance behind the barrier (near y/a_o=150) while above 0.75 employing single scattering hypothesis, which is 2 times of multiple scattering hypothesis computation (m=4). This result illustrates that the displacement amplitude increases at least 100 percent than the actual practice while employing single scattering hypothesis. Admittedly, it should not be ignored while designing barriers.

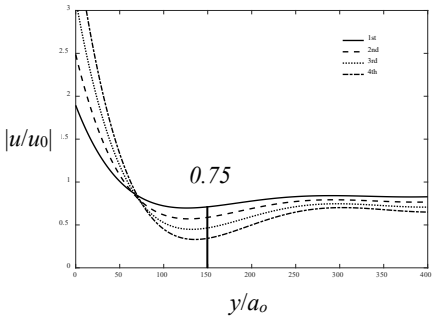

Fig. 3. Dimensionless midline displacement amplitude $|u/u_0|$ behind single-row infilled cavities barrier with the variation of scattering orders ($1 \le m \le 4$)

4.2 The effect of intervals between infilled cavities

It is obvious in Fig. 4 that the dimensionless displacement amplitude behind the center ($0 \le y/a_o \le 100$) of barrier exist amplification appearance. Meanwhile, with the increase of the distance between cavity rows, the displacement amplitude begins to attenuate radially. In a major range behind the barrier, it can isolate more than 40 percent of incident waves. Secondly, with the aggrandizement of intervals between infilled cavities ($2.5 \le s_p/a_o \le 3.5$), the shield effect drops gradually and the best isolation area is close to the barrier ($100 \le y/a_o \le 250$). It is because of increasing the interval between infilled cavities results in the opportunities' increment of incident waves' penetration. Accordingly, it should be considered choosing the infilled cavities' interval s_p/a_o from 2.5 to 3.0 while designing the barriers.

4.3 The effect of the row spacing

Fig. 5 investigates the influence effect of row spacing variation. The value of s_p/a_o is adopted as 3.0 as well for its better isolation effect. Compared Fig. 5 (a) with Fig. 5 (b) (c), the best isolation area appears on the back of cavity rows ($0 \le y/a_s \le 100$) , it blocks more than 80 percent range of incident waves behind the barriers while h=3.0a_s. When the parameters are all constant except increasing the row spacing in a certain range, it can obviously fortify the isolating effect, which is an effective way of adding the barrier thickness and changing the arrangement of cavity rows actually. Secondly, differing from the result of aggrandizing the interval between cavities, increase of row spacing can enhance the shield effect of cavity. It keeps invariant until the distance h/a_o comes to a certain value at 3.5 (in Fig. 5(c)), and the dimensionless displacement amplitude will increase gradually. Thus the row spacing of multi- rows barrier can be acquired a better shield effect in a certain area (the value of h/a_o reaches around 3).

CONCLUDING REMARKS

Based on Biot's saturated medium model and multiple scattering theory, it is solved the scattering problem for plane P-waves about random arrangement and random diameter of infilled cavity in saturated soil. The numerical calculation show that:

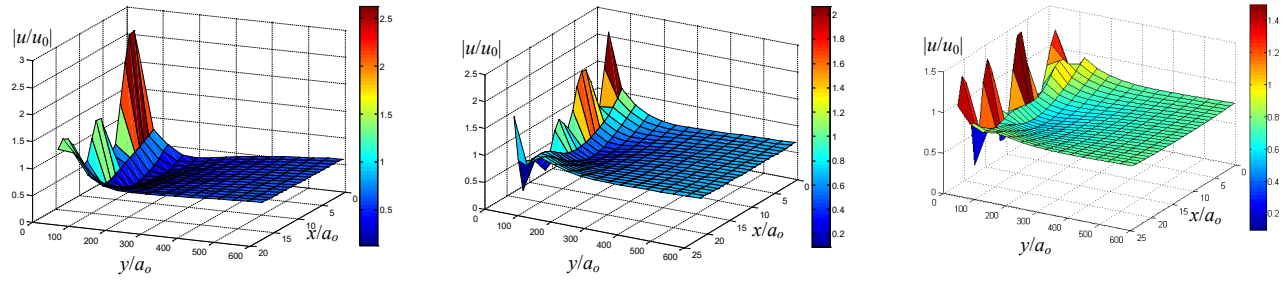

(a) s_p=2.5a_o, h=3.0a_o (b) s_p=3.0a_o, h=3.0a_o (c) s_p=3.5a_o h=3.0a_o

Fig. 4. $|u/u_0|$ surfaces behind hexagon double-row infilled cavities barrier with the variation of intervals s_p (m=4)

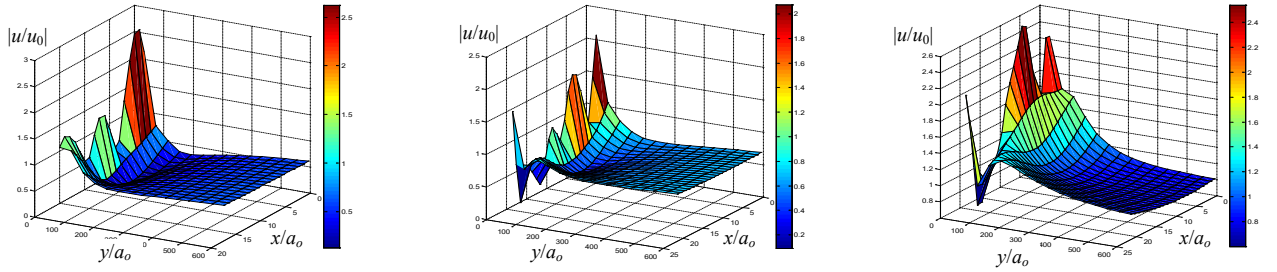

(a) s_p=3.0a_o h=2.5a_o (b) s_p=3.0a_o h=3.0a_o (c) s_p=3.0a_o h=3.5a_o

Fig. 5. $|u/u_0|$ surfaces behind hexagon double-row infilled cavities barrier with the variation of row spacing h (m=4)

(1) The assumption of multiple scattering fills the gaps about ignoring subsequent scattering wave's coherence scattering in the single scattering hypothesis formerly. It acquires higher computational accuracy while intercepting scattering orders m at 4.

(2) The increase of cavity spacing leads to weaken the isolation effect, and the best isolating area also keeps away from the cavity barrier, which resulted from the wave transmitted opportunity increasing. It is advisable to choose the cavity spacing, s_p/a_o between 2.5 to 3.5 and the row spacing h/a_o between 3.0 to 3.5 while designing barriers.

ACKNOWLEDGEMENTS

The authors are grateful to Chinese Institution of Soil Mechanics and Geotechnical Engineering for providing this precious chance, and thanks to all the anonymous reviewers for their helpful advices and valuable comments. The work described in this paper was supported by the Zhejiang Provincial Natural Science Foundation of China (Grant No. LY18E080024) and National Science Foundation of China (Grant No. 51408549).

REFERENCES

[1] Pao, Y. H. and Mow, C. C. (1973). Diffraction of Elastic Waves and Dynamic Stress Concentrations. Crane Russak, New York, USA.

[2] Avilés, J. and Sánchez-sesma F. J. (1983). Piles as barriers for elastic waves. Journal of Geotechnical Engineering, 109(9), 1133-1146.

[3] Hu, Y. Y., Wang, L. Z. and Chen, Y. M., et al. (1998). Scattering and refracting of plane strain wave by a cylindrical inclusion in fluid saturated soils. Earthquake Science, 11(3), 87-95.

[4] Stoll, R. D. (1998). Reflection of acoustic waves at a water-sediment interface. Journal of the Acoustical Society of America, 70(1), 149-156.

[5] Cai, Y. Q., Ding, G. Y. and Xu, C. J. (2009). Amplitude reduction of elastic waves by a row of piles in poroelastic soil. Computers & Geotechnics, 36(3), 463-473.

[6] Cai, Y. Q., Ding, G. Y. and Xu, C. J., et al. (2010). Vertical amplitude reduction of Rayleigh waves by a row of piles in a poroelastic half-space. International Journal for Numerical & Analytical Methods in Geomechanics, 33(16), 1799-1821.

[7] Xu, P., Tie, Y. and Chen, B. (2015). Isolation of fast longitudinal waves by barriers composed of several rows of cylindrical cavities in saturated soils. Journal of Vibration and Shock, 34(16), 73-78.

[8] Xu, P., Deng, Y. H. and Wu, M. (2014). Isolation of fast compressive waves by barriers composed of several rows of piles saturated soils. Engineering Mechanics, (5), 120-127.

[9] Xia, T. D., Chen, C. and Sun, M. M. (2011). An improved method for multiple scattering under SV incident waves and vibration isolation using rows of piles. Journal of Vibration and Shock, (4), 86-90.

[10] Xia, T. D., Sun, M. M. and Chen, C. et al. (2011). Analysis of Multiple Scattering by an Arbitrary Configuration of Piles as Barriers for Vibration Isolation. Soil Dynamics and Earthquake Engineering, 31(3), 535-545.

[11] LU, J. F., ZHANG, X. and LI, C. X. (2014). Vibration isolation system for linked pile rows and its numerical simulation. Chinese Journal of Geotechnical Engineering, 36(7), 1316-1325.

[12] Lu, J. F., Zhang, X. and Zhang, R. (2014). A wavenumber domain boundary element model for the vibration isolation via a new type of pile structure: linked pile rows. Archive of Applied Mechanics, 84(3), 401-420.

[13] Sun, M. M. (2014). Multiple scattering of SH waves by rows of arbitrarily arranged tubular piles. Rock and Soil Mechanics, 46(4), 943-950.

[14] Sun, M. M., Zhang, S. M. and Tan, Z. F. et al. (2018). Multiple scattering of P waves by rows of cavities as barrier with arbitrarily arranged in saturated soil. Journal of Natural Disasters, 27(2), 24-32.

[15] Wu, S. M. (1997). Wave propagation in soils. Science Press, Beijing, China.